2007 IEEE International Conference on
Robotics and Automation
Roma, Italy, 10-14 April 2007

Teleoperation of Steerable Needles

Joseph M. Romano, Robert J. Webster III, and Allison M. Okamura

***Abstract*— Needles are commonly used in medical practice as a minimally invasive means to reach subsurface targets for diagnosis or therapy delivery. Recent results indicate that steerable needles may enhance targeting accuracy and allow needles to avoid obstacles along the path to the target. This work considers teleoperation of needles made of a superelastic alloy that steer through tissue using forces generated by the standard asymmetric bevel tip. The needle may be modeled as a nonholonomic system, with inputs of insertion along and spin about the needle axis. A teleoperation system consisting of a commercial master haptic device, a custom needle-steering robot slave, and visual feedback to the operator was assembled. Human subjects experiments were performed to evaluate targeting accuracy in phantom tissue for three needle control methods: teleoperation of both insertion and spin, teleoperation of insertion with open-loop-controlled spin, and open-loop control of both insertion and spin. Targeting accuracy improved with increasing degrees of freedom of human (teleoperation) control, primarily because tissue deformation and modeling limitations result in open-loop control errors. Subjects typically performed multiple spins of the needle during insertion in order to fine tune the needle path. In addition, position, rate, and a nonlinear hybrid control were compared during teleoperation of the insertion degree of freedom. The hybrid method resulted in significantly better targeting accuracy.**

I. Introduction

Needle insertion is an important aspect of many medical diagnoses and treatments, particularly percutaneous procedures requiring therapy delivery or sample removal. However, errors in final tip placement mitigate the effectiveness of diagnosis or therapy, and cannot be corrected without the ability to steer the needle inside tissue. Examples include biopsies taken from the wrong location which produce false negative cancer diagnoses, and prostate brachytherapy, where radioactive seeds rarely reach locations pre-planned for optimal dosage. Steering capability can can also allow needles to travel around vital anatomical structures that block straight-line access to the desired final tip target.

Model-based or teleoperative control and planning for steerable needles can compensate for disturbances due to needle bending, error in insertion angle, and tissue deformation. In this paper, we consider the teleoperation of very flexible needles with beveled tips. The bevel acts as a wedge causing the needle to deflect as it enters tissue (Figure 1), with the direction of deflection controlled by rotating the needle about its axis. In [14], we presented a nonholonomic model to describe the needle tip pose as a function of two inputs, insertion velocity and angular velocity of the bevel about the needle axis. Using this model, along with mechanical and geometric tissue properties, it is possible to plan optimal paths to reach a desired target [1], [2], [3].

This material is based on work supported by NSF Grant #EIA-0312551 and NIH Grant #R21 EB003452.

J. M. Romano, R. J. Webster III, and A. M. Okamura are with the Department of Mechanical Engineering, The Johns Hopkins University, Baltimore, Maryland, 21218, USA {jromano6, robert.webster, aokamura}@jhu.edu.

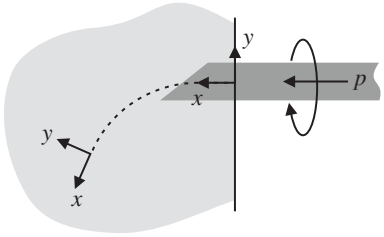

Fig. 1. As a flexible needle is inserted into tissue along its axis (x), the tip deflects. Spinning the needle about its axis (θ) will change the steering direction, allowing the tip to reach any pose in the workspace.

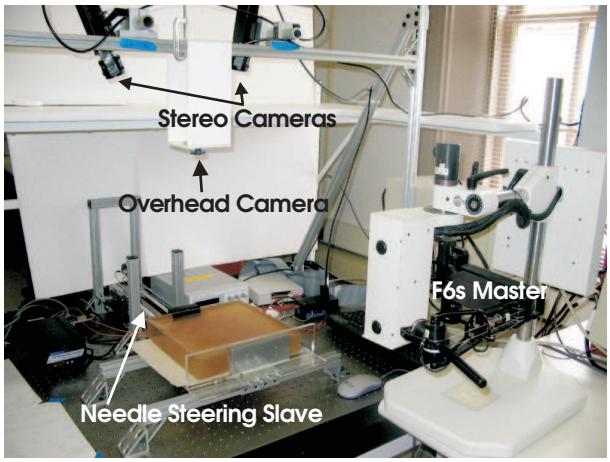

Fig. 2. Complete needle teleoperation system. Components pictured include the slave JHU Needle Steering robot [15], the master Freedom 6S robot [4], calibrated stereo cameras to record needle position, and an overhead camera to capture images displayed to the user.

While the nonholonomic model can describe the path of the needle in fairly homogeneous phantom tissues (e.g. blocks of silicone rubber or porcine gelatin), it will never be perfect for living tissues, due to their inherent variability and unpredictable effects of boundary layers and bleeding. To address these model limitations, we are considering several complementary approaches. A first approach is a low-level closed-loop image-based control system, which is presented in [9]. A second approach is high-level re-planning based on image feedback. These methods would allow completely autonomous needle control, once the target and obstacles are defined by the surgeon. The focus of this paper is a third approach, teleoperation. In this system, the human operator

(a surgeon) provides real-time position or rate commands that are followed as closely as possible by a slave robot.

Teleoperation offers both advantages and disadvantages in comparison to autonomous, closed-loop control methods. A primary advantage is that it allows the surgeon to have closer control over the needle motion. For reasons of safety and acceptance by the medical community, this close interaction may be needed for initial clinical trials. A disadvantage is the difficulty humans have in planning and following paths with nonholonomic systems. In comparison to hand-held needle insertion, teleoperation can enhance steerability because the robot can use needles that would be far too flexible to accurately insert by hand. Needle insertion (even without steering) is very difficult without computer assistance, since it requires the physician to have excellent 3D spatial reasoning, extensive experience, and precise coordination with high-resolution real-time image feedback. We propose that the best teleoperation method is a mixed approach, where the human controls the invasive degree of freedom (DOF), insertion, while the computer controls the steering by spinning the needle about its axis. This paper describes our teleoperation system design, experiments to examine the performance of needle insertion under different levels of human control, and results comparing control methods and needle steering strategies.

A. Related Work in Needle Steering

Clinically, needles are manually steered through a combination of lateral, twisting, and inserting motions under visual feedback from imaging systems such as ultrasound. However, these techniques can yield inconsistent results and are difficult to learn. Physicians also sometimes attempt to prevent bending by continually spinning bevel tip needles during insertion.

Our bevel steering method described above [14] has been adopted and the maximum achievable curvature increased using different needle tip shapes and sizes by a group at Carnegie Mellon University [6]. Lateral motion and tissue deformation can also cause steering, and other research groups have modeled those effects [5], [8]. Other strategies include incorporating a curved stylus inside a straight cannula [11] and using multiple prebent cannulas (e.g. [16], [12]). Ultimately, we expect that some combination of the above approaches – needle flexibility, bevel asymmetry and shape, prebent elements, needle base actuation and possibly tissue manipulation – will lead to a system with superior steering capability in actual soft tissue over any one method alone.

B. Related work in Teleoperation

In addition to specific work on needle steering, there are a number of examples in the literature of robot-controlled needle insertion [13], many of which are teleoperated with simple computer interfaces such as mice, keyboards, and joysticks. The input devices in this prior work differ from our system because they are used to control the orientation of the needle *before* it is inserted into tissue, and only move the needle along its axis after insertion. There are also teleoperation systems for robot-assisted catheter insertion, e.g. Hansen Medical, Inc. (Mountain View, CA, USA), which do not operate under the same kinematic constraints as our needle steering system.

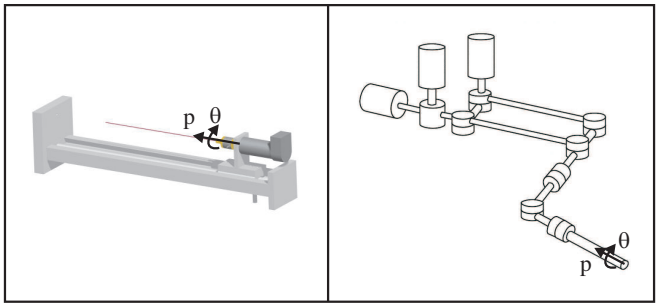

Fig. 3. The correspondence of slave robot DOF (left) and master robot DOF (right) for teleoperation.

Our needle steering teleoperation work is more closely related to teleoperation of nonholonomic systems, such as wheeled mobile robots. Researchers have developed control methods for telemanipulation of mobile robots with joysticks, e.g. [10], [7]. In these systems, the input degrees of freedom (typically left/right and up/down) are not kinematically similar to the mobile robot motion (e.g. they might adjust wheel speeds for a 2-wheeled skid-steered mobile robot). In this paper, we match the needle insertion degree of freedom to translational motion of the master stylus, and the needle spin degree of freedom to the spin of the stylus. As far as the authors are aware, there is no prior work comparing different degrees of freedom of operator control versus autonomous control for teleoperated nonholonomic systems.

II. Needle Steering Teleoperation System

In order to perform needle steering teleoperation experiments, we designed the novel hardware and software system shown in Figure 2. The JHU needle steering robot is used as a teleoperated slave robot, as shown in Figures 2 and 3. It controls the two input DOF of the steerable needle: translation to push the needle into tissue, and the axial rotation used to reorient the bevel tip. The robot prevents buckling of the superelastic needle outside the tissue using a telescoping antenna sheath.

To teleoperate the slave robot, the user grasps the pen-like stylus of the Freedom 6S (F6S) [4], a commercial haptic device from MPB Technologies, Inc. (Montreal, Canada). Stylus axial rotation is mapped to needle axial rotation, and the horizontal translation of the stylus (with respect to the F6S base frame) is mapped to the translation of the needle as shown in Figure 3. Since the base of the needle cannot translate in the y or z directions, translation of the F6S along the y and z axes of its base frame was similarly constrained (using virtual springs) to a line parallel to the F6S base frame x axis.

Two Sony XCD-X710 Firewire Cameras running at a resolution of 1024 $\times$ 768 were calibrated for stereo image

analysis in order to record needle tip positions in three dimensions. A version of the well-known SSD tracking algorithm is used to process images, extracting needle tip position with an update rate of approximately 5 Hz. Using high resolution cameras and accounting for light refraction at the tissue surface, we achieved position measurement accuracy of 2 mm. This tip position data is recorded for analysis and also transmitted to visual displays that assist the user in performing the insertion task as described below. A third camera, an ADS Technologies Pyro Firewire Webcam, provides a real-time view of the needle to the user.

All experiments reported in this paper were performed using a cylindrical nitinol needle with a diameter of 0.6 mm and a bevel angle of 45°. The phantom tissue used for the experiments was Super Soft Plastic from M-F Manufacturing, Inc (Ft. Worth, TX, USA). The rubber-like Super Soft Plastic was molded into a rectangular prism 28 × 28 × 4 cm.

A. Visual Feedback

In addition to an overhead camera view, the user was provided with two additional visual aids as shown in Figure 4. While the overhead camera provides a visual indication of needle position in two dimensions, it does not show depth. Thus, we provided a depth meter in the form of a slider that displays the vertical depth of the needle tip with respect to the top and bottom surfaces of the tissue (in the z direction as shown on Figure 4).

Since the bevel tip is too small to visualize clearly in camera images, we also provided a second visual aid to the user to indicate bevel direction. A dial gauge indicates the direction the needle will curve (in the needle tip frame) as it translates forward, by displaying the reading of an encoder attached to the needle base. At the initial needle configuration, when the arrow is pointing towards 90°, insertion will cause the needle to curve in the plane of the tissue toward the positive y direction, as shown in Figure 4. An angle of 270° will make the needle curve in the opposite direction. Readings of 180° and 0° make the needle go up or down in the z direction, respectively. While the encoded base rotation may not perfectly correspond to tip rotation due to friction and finite torsional stiffness of the needle shaft, it is a good approximation – especially at shallow depths. Additionally, we expect the blood in human tissue to form a natural lubricant, making torsional deformation even less significant than in rubber phantoms.

B. Control Methods

The purpose of our study was to examine the effect of various translational degree of freedom control methods on user performance of targeting tasks, and also to compare user performance for several variants of human versus automatic open-loop control. The correspondence of degrees of freedom between the master and the slave was maintained as shown in Figure 3 for all experiments.

The teleoperation of needle spin was accomplished through a proportional-derivative control law,

$$\tau_n = k_p(\theta_m - \theta_s) + k_d\dot{\theta}_s, \tag{1}$$

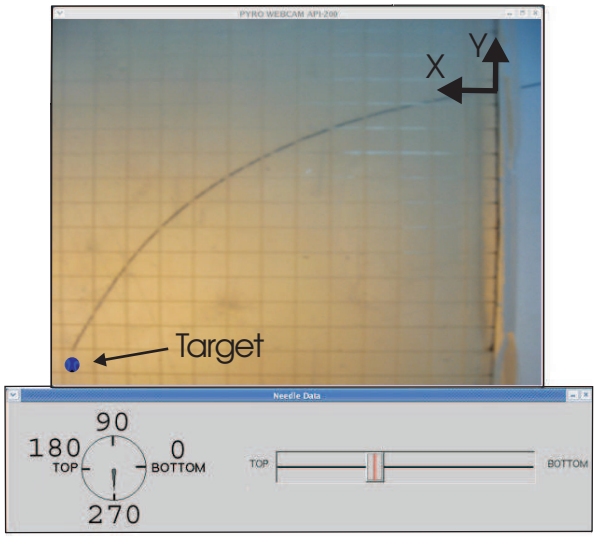

Fig. 4. Operator feedback graphics window. The overhead camera view (top), direction gauge (bottom left), and depth meter (bottom right) can all be seen simultaneously by the user.

where θ_m and θ_s are the angles of the master stylus and slave needle/motor, respectively, k_p and k_d are the proportional and derivative gains, with values of 6.02 mN-m and 0.0602 mN-m-s respectively. τ_n is the torque applied to the needle by a DC brushed motor. The translational motion of the needle is generated by a stepper motor and lead screw. The stepper motor has its own low-level controller, which may accept either position or velocity commands. Three different methods were used to compute these commands, as described in the following subsections.

1) Position Control: The first translational control method was a position controller:

$$p_s = k_1 p_m, \tag{2}$$

where p_m is the position of the master stylus, p_s is the desired position of the slave needle (transmitted to the low-level stepper motor controller), and k_1 is a unitless scalar gain of 0.7. The gain k_1 sets the fixed scaling between the master and slave positions. There is a tradeoff between fast response and accuracy in selecting k_1. Low values allow fine position control, but require the master to move a great distance to achieve appreciable slave motion. For our system, 0.7 seemed to yield the best accuracy for a reasonable distance of master motion. Also, users were allowed to "clutch" the system. Motions made in the direction of retraction were ignored, allowing the user to reposition the stylus for further insertion. This effectively increased the workspace of the master. Preventing backward motion also allowed us to limit the variation in user strategies for reaching the target, although users were still free to spin the needle as much as desired.

2) Rate Control: Rate control allows the user to command the velocity of the slave. We implemented it using the

following relationship,

$$v_s = k_2 p_m, \tag{3}$$

where k_2 is a scalar gain with a value of 0.052, and units of 1/sec. A point near the center of the F6S workspace was set as the zero position of the x-axis. Translations of the master to the left (positive x direction) result in needle insertion into the tissue. A virtual spring-damper force feedback system was implemented on the master to pull the operator back to the zero position, as is commonly done in rate-control input devices. Retractions of the needle were disallowed by ignoring displacement in the negative x direction.

3) Hybrid Control: To create a system that simultaneously enables long quick motions, yet maintains the ability to do fine positioning in the vicinity of the target, we developed a hybrid control law. This was based on inspiration from the most ubiquitous user input device, the computer mouse. The scaling feature in computer mice is known as mouse ballistics, and is a standard method for moving pointers around computer screens. It inspired the following hybrid needle control law,

$$v_s = k_3 v_m^2, \tag{4}$$

where k_3 is a scalar gain with a value of 21.6 and units of sec/m. This nonlinear control law causes slow motions of the master to produce fine-resolution movements of the slave regardless of workspace position, but also enables the slave to move faster when the master is moved quickly.

III. Teleoperation Experiments

To test the effect of the control methods described above on user performance in reaching specific targets, we conducted a series of experiments. Subjects were instructed to perform a series of targeting tasks to reach two different points in the needle's workspace – one near its edge and one near its center – requiring different strategies to reach them. Target 1 was selected as the average point reached by the needle tip in the x-y plane in eight 12 cm insertions with a fixed bevel direction of 90°, at a fixed velocity of 6.35 cm/s. Target 2 was selected as the average point reached by the needle tip in the x-y plane in eight 13 cm insertions at the same velocity, where the bevel tip was first fixed at 90°, then inserted 6.5 cm, then rotated to 270°, and finally inserted another 6.5 cm. In order to view the needle tip in the camera image and initiate tip tracking, the starting point for all insertions was at a depth of 2 cm inside the phantom tissue. The needle was moved to this position by first inserting 1 cm with the bevel angle was fixed at 0°, and then inserting 1 cm with the bevel angle was fixed at 180°. All data reported (including the selection of target positions) starts from this 2 cm position inside the tissue.

For each trial, the control method was described to the user and he or she performed an unrecorded practice run to become accustomed to the system. The user was instructed to position the needle tip as close as possible to the target in the x-y plane, and perform the task as swiftly as possible without sacrificing position accuracy. During the practice run, users were instructed to navigate to one of the two targets described above, while the experimenter provided assistance (primarily, pointing out the proper interpretation of the graphical feedback). After the practice run, the system was reset to the starting conditions and the users were then told to repeat the task for the recorded trial. The recorded trials were identical to the sample run, with the exception that no assistance was provided by the experimenter. After navigating to one target under a given control law, the target was then changed and the trial repeated with the user being instructed to navigate to the new point. The control law was then changed, and the above sequence of explanation, practice run, and recorded trial was repeated. The order of presentation of the three control laws was varied randomly among the users to remove any potential learning effect from the results.

Our nomenclature for the control conditions presented to the user is of the form [letter][letter][number]. The first letter denotes the control law used for the translational motion with 'P' indicating the position control law (Equation 2), 'R' indicating rate control (Equation 3), H indicating the hybrid control (Equation 4), and A indicating automatic insertion at a fixed velocity by the computer. The second letter denotes whether the rotation stage was controlled by the human operator (denoted 'H') or controlled automatically by the computer (denoted 'A'). The final number in our nomenclature refers to the specific target point, '1' for Target 1, and '2' for Target 2. For example, PH1 should be interpreted as position control of translation, human control of axial needle rotation, and Target 1 as the objective.

A total of 14 subjects, from 18 to 27 years of age, performed the experiments described above. Experience in teleoperation ranged from novice to expert, a range that closely approximates the varying level of teleoperation experience of surgeons. Since steering flexible needles (especially via teleoperation) is significantly different from inserting rigid steel needles by hand, we did not require subjects to have experience in hand-insertion to qualify for our study. To keep the each subject's experiment duration below one hour, each subject performed a subset of all combinations of trials listed above. All subjects attempted RH1, RH2, RA1, RA2 with one trial each. For PH1, PH2, PA1, PA2, HH1, HH2, HA1, and HA2 subjects were alternated between position and hybrid control, performing all permutations of only one of the two. That is, if a user performed PH1, she would not perform HH1, and vice versa.

IV. Results

The effect of different control methods on the targeting accuracy of the subjects was determined from data collected by the stereo cameras. The error metric used to evaluate the targeting accuracy was the x-y distance of needle tip from the target ($e = \sqrt{\delta x^2 + \delta y^2}$). We did not include depth (z) in our error metric because the main goal specified to subjects was to reach the correct x-y position, with maintaining constant depth being a secondary objective. We did not restrict needle motion to a specific plane because this

	RH1	PH1	HH1	RA1	PA1	HA1	AA1	
RH2			y	y	y	y	y	RH1
PH2			y	y	y	y	y	PH1
HH2	y	y		y	y	y	y	HH1
RA2	*	*	y					RA1
PA2	*	*	y					PA1
HA2	*	*	y					HA1
AA2	*	*	y					AA1
	RH2	PH2	HH2	RA2	PA2	HA2	AA2	

Fig. 5. Scheffe test results for a single factor ANOVA of varying control methods vs. radial distance from needle tip to target. 'y' represents a statistical difference in means with a confidence greater than 95%, '*' means a confidence between 85% and 95%, and a blank space means a confidence lower than 85%.

would require closed-loop control of tip position, and such controllers are not yet available, despite promising initial results [9]. Simply restricting the angular rotation of the needle to two discrete values 180° apart would not account for tissue inhomogeneity and finite torsional stiffness of the needle shaft.

A. Targeting Accuracy

To evaluate user targeting performance, we performed a single-factor, one-way, random effects ANOVA. The independent variable was the control method used and the dependent variable was the error metric. This enables a statistical comparison of improvement in user performance of our targeting tasks. Figure 5 presents the statistical significance of pairwise comparisons, determined using a Scheffe test. Figures 6 and 7 show the average and standard deviation of the targeting error resulting from the various control methods. The columns $AA1$ and $AA2$ represent the fully automated case, where the computer controlled both rotation and insertion of the needle open-loop.

The clearest result of these experiments is that the new hybrid control law enabled users to target more accurately than any other controller. This validates our hypothesis that a controller inspired by mouse ballistics can improve teleoperated needle steering accuracy over more traditional rate and position control methods. We attribute this increase in accuracy to the seamless scaling between rapid movements and fine positioning control of the hybrid control law. Using rate control, users often accidentally deviated very early in the trial from the correct family of possible trajectories too significantly to recover before reaching the target depth. Conversely, using position control, users navigated successfully to the area near the target, but were incapable of fine-tuning their position within this area. This is as one would expect for the linear position and rate control mappings, in contrast to the nonlinear mapping of hybrid control.

The data also shows that human control of needle spin can be statistically significantly more accurate than fully automated open-loop control. We attribute this to human compensation for a number of sources of uncertainty in needle tip position that produce variation in trials with the same input joint angle profiles. Among these factors are (1) inhomogeneity of the phantom tissue (present to some degree despite it being cast from a single batch of Super Soft Plastic), (2) initial deflection of the needle upon "popping through" the rubber surface (the "nuisance parameters" described in [14]), and (3) small errors in calibrating the initial zero rotation angle of the bevel-tip. Under open loop control, all of these sources of error cause deviations from the expected needle endpoint. As one would expect, the human reduces the effect of these sources of error by servoing the system toward the target.

B. User Strategy for Task Completion

As described above, Target 2 was achieved in the fully automatic trials by generating an 'S' shape by making a single 180° rotation of the bevel angle half way through the insertion. It is interesting to note that most human subjects tended to use insertion strategies composed of 3 to 5 180° turns when attempting to reach the same target point as shown on the histogram in Figure 8. Figure 9 shows several example user paths taken to reach the target, as well as one open-loop computer controlled trial.

V. Conclusions

Needle steering has many advantages over current clinical practice, in which needles follow only nominally straight-line trajectories and there is no means of compensating for errors

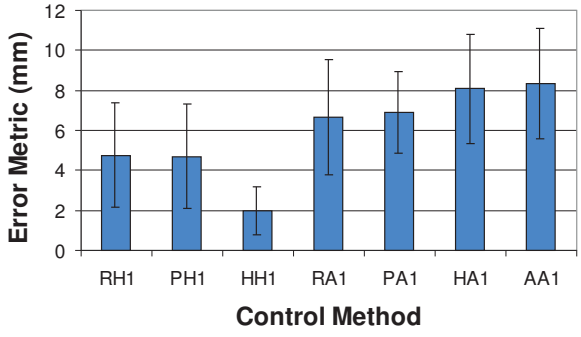

Fig. 6. Mean and Standard Deviation of the radial distance from needle tip to target for various combinations of control methods to reach target 1.

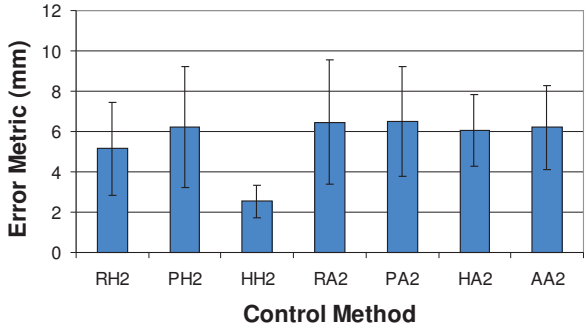

Fig. 7. Mean and Standard Deviation of the radial distance from needle tip to target for various combinations of control methods to reach target 2.

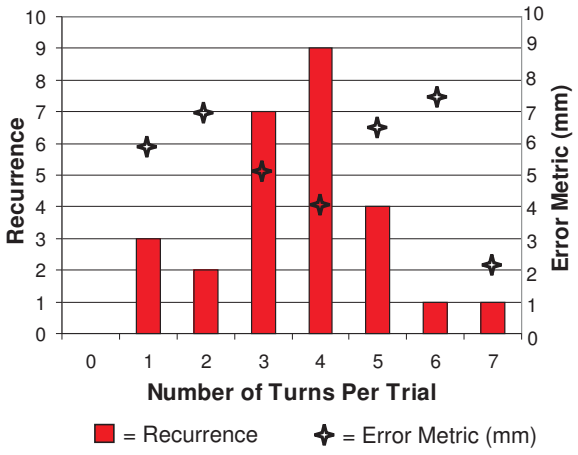

Fig. 8. (Left Axis) Histogram of the number of users performing n turns. (Right Axis) The average radial distance from the needle to tip to the target point for users performing n turns, denoted by '+'.

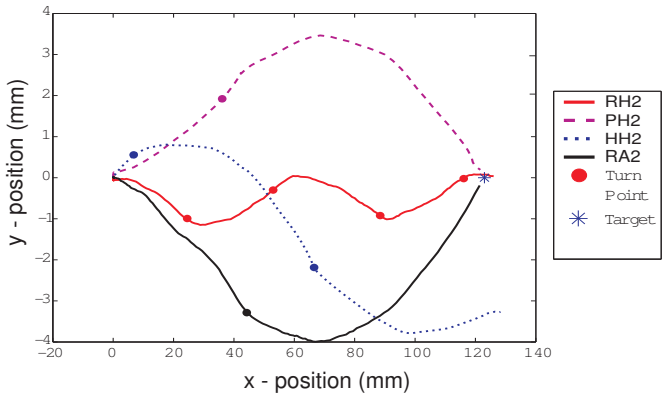

Fig. 9. Users applied different strategies for reaching Target 2. Most users invoked more axial spin of the needle than the computer-controlled case.

induced by imperfect alignment, tissue deformation, etc. For clinical acceptance and safety reasons, allowing the surgeon to remain "in the loop" during the procedure is desirable. We conducted human subjects experiments to evaluate targeting accuracy in phantom tissue for three steerable needle control methods: teleoperation of both insertion and spin, teleoperation of insertion with open-loop-controlled spin, and open-loop control of both insertion and spin. The hybrid control law resulted in significantly better targeting accuracy. Targeting accuracy also generally improved with increasing number of degrees of freedom of human (teleoperation) control, primarily because the human compensated for errors like tissue deformation and other unmodeled effects. In future work, we plan to use closed-loop image-based control to replace the open-loop automatic control. In that case, it may be possible to achieve better performance from computer-controlled needle insertion than human teleoperated needle insertion, and teleoperation of insertion with closed-loop-controlled spin may be the best possible practical compromise for initial clinical use of steerable needles.

VI. Acknowledgments

The authors thank Noah Cowan for insightful conversations regarding controllers, Vinutha Kallem for providing needle tracking software, and Robinson Seda and Katie Zhuang for their support in manufacturing the needle and phantom tissue, as well as Noah Cowan, Gregory Chirikjian, Ron Alterovitz, and Ken Goldberg for their contributions to needle steering model development and path planning.

References

[1] R. Alterovitz, M. Branicky, and K. Goldberg. Constant-curvature motion planning under uncertainty with applications in image-guided medical needle steering. In *Workshop on the Algorithmic Foundations of Robotics*, July 2006.

[2] R. Alterovitz, K. Goldberg, and A. Okamura. Planning for steerable bevel-tip needle insertion through 2D soft tissue with obstacles. In *Proc. IEEE Int. Conf. on Robotics and Automation*, pages 1652–1657, Apr. 2005.

[3] R. Alterovitz, A. Lim, K. Goldberg, G. S. Chirikjian, and A. M. Okamura. Steering flexible needles under markov motion uncertainty. In *Proc. IEEE/RSJ Int. Conf. on Intelligent Robots and Systems*, pages 120–125, Aug. 2005.

[4] J.-G. S. Demers, J. M. A. Boelen, and I. P. W. Sinclair. Freedom 6s force feedback hand controller. In *SPRO '98 IFAC Workshop on Space Robotics*, Montreal, Canada, October 19-22 1998.

[5] S. P. DiMaio and S. E. Salcudean. Needle insertion modeling and simulation. *IEEE Transactions on Robotics and Automation*, 19(5):864–875, 2003.

[6] J. A. Engh, G. Podnar, D. Kondziolka, and C. N. Riviere. Toward effective needle steering in brain tissue. *28th Annual International Conference of the IEEE Engineering in Medicine and Biology Society*, pages 559–562, 2006.

[7] R. B. Gillespie, J. E. Colgate, and M. A. Peshkin. A general framework for cobot control. *IEEE Transactions on Robotics and Automation*, 17(4):391–401, 2001.

[8] D. Glozman and M. Shoham. Flexible needle steering and optimal trajectory planning for percutaneous therapies. In *Medical Image Computing and Computer-Assisted Intervention - MICCAI*, pages 137–144, 2004.

[9] V. Kallem and N. J. Cowan. Image-guided control of flexible bevel-tip needles. *IEEE International Conference on Robotics and Automation*, 2007. (in press).

[10] V. Mut, J. Postigo, E. Slawinski, and B. Kuchen. Bilateral teleoperation of mobile robots. *Robotica*, 20:213–221, 2002.

[11] S. Okazawa, R. Ebrahimi, J. Chuang, S. E. Salcudean, and R. Rohling. Hand-held steerable needle device. *IEEE/ASME Transactions on Mechatronics*, 10(3):285 – 296, 2005.

[12] P. Sears and P. Dupont. A steerable needle technology using curved concentric tubes. *IEEE/RSJ International Conference on Intelligent Robots and Systems (IROS)*, pages 2850–2856, 2006.

[13] D. Stoianovici, R. Webster, and L. Kavoussi. Surgical robotic applications in minimally invasive uro-oncology surgery. In *Minimally Invasive Uro-Oncologic Surgery*, pages 353–363. London & New York: Taylor & Francis, 2005.

[14] R. J. Webster III, N. J. Cowan, G. S. Chirikjian, and A. M. Okamura. Nonholonomic modelling of needle steering. *International Journal of Robotics Research*, 25(5/6):509–526, May/June 2006.

[15] R. J. Webster III, J. Memisevic, and A. M. Okamura. Design considerations for robotic needle steering. *IEEE International Conference on Robotics and Automation*, pages 3599–3605, 2005.

[16] R. J. Webster III, A. M. Okamura, and N. J. Cowan. Toward active cannulas: Miniature snake-like surgical robots. *IEEE/RSJ International Conference on Intelligent Robots and Systems (IROS)*, pages 2857–2863, 2006.